J. Cosmet. Sci., **65,** 175–186 (May/June 2014)

Effect of novel cyclohexane diester and benzene diester derivatives on melanogenesis

JONG WOO CHEON, JI MIN JEON, MOON JEONG CHOI, SI JUN PARK, and SANG YO BYUN, *R&D Center, ACT Co., Ltd., 486 Sin-dong (J.W.C., J.M.J., M.J.C., S.J.P.), Suwon, Republic of Korea and Cosmetic Science Major, Department of Applied Biotechnology, Ajou University, Woncheon-dong (J.W.C., S.Y.B.), Suwon 443-749, Republic of Korea.*

Accepted for publication March 20, 2014.

Synopsis

In order to investigate potent whitening agents, we synthesized 15 cyclohexane diester derivatives and 15 benzene diester derivatives. To evaluate their structure–cytotoxicity relationships, we performed cell cytotoxicity tests on B16F10 mouse melanoma cells. To understand their whitening effects, melanin synthesis inhibitory activities in B16F10 cells and mushroom tyrosinase inhibitory activities were performed. In most cases, cell cytotoxicity was observed to be lower in 1,3-diester than in 1,2- and 1,4-diesters; when it came to the structural isomer of the side chain, all derivatives except the 1,2-cyclohexane diester derivatives showed lower cell cytotoxicity in the branch type of the side chain than in the linear type. Among the compounds evaluated, the compounds cyclohexane-1,3-diyl bis(decanoate), cyclohexane-1,4-diyl dioctanoate, and 1,3-phenylene bis (2-ethylhexanoate) emerged as potent melanin synthesis inhibitors. Our goal was to determine the expression levels of proteins involved in melanogenesis, Western blotting and RT-PCR showing that these compounds decreased tyrosinase, TRP-1, and TRP-2 while demonstrating significantly low cytotoxicity.

INTRODUCTION

Melanin is a major pigment produced by melanocyte cells in the basal layer of human skin and overproduced by chronic sun exposure or other hyperpigmentation diseases (1). Melanin synthesis is regulated by the rate-limiting enzyme of tyrosinase, which is a membrane-bound copper containing glycoprotein that initiates the biosynthetic pathway of melanin by catalyzing the hydroxylation of tyrosine to 3,4-dihydroxyphenylalanine (DOPA). Subsequent reactions in the melanin synthetic pathway—for example, the conversion of DOPA to DOPAquinone as well as other non-enzymatic reactions—are oxidative reactions (2). Tyrosinase is known to be a key enzyme for melanin biosynthesis in plants, microorganisms, and human cells. Against this backdrop, many tyrosinase inhibitors have been tested in cosmetics and pharmaceuticals as a way of preventing any overproduction of melanin in epidermal layers (3).

Address all correspondence to Jong Woo Cheon at actcjw@actcos.com.

Benzenediols in hydroxyl groups are substituted onto a benzene ring. Benzenediols have three isomers: Catechol is commonly known as 1,2-benzenediol (*ortho*-isomer); resorcinol is 1,3-benzenediol(*meta*-isomer); and hydroquinone is 1,4-benzenediol (*para*-isomer). Tyrosinase (EC 1.14.18.1) contains two copper atoms in its active site and binds dioxygen to give oxy-tyrosinase. This form of the enzyme catalyzes *ortho*-quinone formation by catechol oxidation. Catechols irreversibly inactivate tyrosinase, where the bound catechol deprotonates, leading to the reductive elimination of Cu(0) from the tyrosinase active site (4,5). The resorcinol substrate is oxidized *via* the monooxygenase route, generating a hydroxyl intermediate that undergoes deprotonation and results in the irreversible elimination of Cu(0) from the tyrosinase active site (6). Hydroquinone is not a primary substrate for tyrosinase. The presence of the *para*-hydroxy group prevents binding to the tyrosinase active site (7). Therefore, the tyrosinase inhibitory activity to treat pigmentation disorders has recently been a major subject in numerous studies (8–10). Kojic acid and arbutin are well-known depigmenting agents. A4-substituted resorcinols have been reported to be potent tyrosinase inhibitors, and their structure–activity relationships and inhibition mechanisms have been examined in detail (11,12) Also, 4,4'-(ethane-1,2-diyl)bis(resorcinol) is known to show a potent tyrosinase inhibitory activity that is almost 20-fold stronger than that of kojic acid (13).

In this study, we discuss the structure–cytotoxicity relationships, the melanin content, and mushroom tyrosinase inhibitory activities of 30 benzene diester derivatives with wide-ranging acyl group (butanoyl, hexanoyl, octanoyl, decanoyl, and 2-ethylhexanoyl) and hydroxyl group disposition in the benzyl part as whitening agents (see Table I for structures). These benzene diester derivatives have not been studied before in this context. The melanogenesis inhibitory activity of a series of benzene diesters is set here against their structure and cytotoxicity. The results will support the design of novel depigmentation agents.

MATERIALS AND METHODS

CHEMICALS AND REAGENTS

The reagents of 1,2-cyclohexanediol, 1,3-cyclohexanediol, 1,4-cyclohexanediol, 1,2-benzenediol, 1,3-benzenediol, 1,4-benzenediol, butyl chloride, hexanoyl chloride, octanoyl chloride, decanoyl chloride, 2-ethylhexanoyl chloride, tetrahydrofuran (THF), triethylamine (TEA), anhydrous magnesium sulfate, L-tyrosine, 3-(4,5-dimethylthiazol-2-yl)-2,5-diphenyltetrazolium-bromide (MTT), dimethyl sulfoxide (DMSO), and all other chemicals were purchased from Aldrich Chemical Co. (St. Louis, Mo). Dulbecco's modified Eagle's medium (DMEM), fetal bovine serum (FBS), penicillin, streptomycin, and trypsin-EDTA were bought from Thermo Scientific Co. (San Francisco, CA). Tyrosinase, TRP-1, and TRP-2 antibodies were obtained from Santa Cruz Biotechnology. (Dallas, TX). PD 98059, H-89, KT 5720, RO-32-0432, and SB 203580 were sourced from Calbiochem (Damstadt, Germany). The reactions were monitored by TLC on silica gel F254 (Merck, Damstadt, Germany). Column chromatography was carried out using 230–400 mesh silica gel (Merck). Proton nuclear magnetic resonance spectra were recorded on a JNM-AL300 (300 MHz; JEOL, Tokyo, Japan) spectrometer with tetramethylsilane as an internal standard. A FT-IR spectrum was recorded on a Scimitar 1000 FTS (Varian, Randolph, MA). SpectraMax 190 (Molecular Devices, Sunnyvale, CA) was used as the absorbance.

Table I
Chemical Structures of Cyclohexene Diester Derivatives (1a–1o) and Benzene Diester Derivatives (2a–2o)

Compounds	R	n	Compounds	R	n
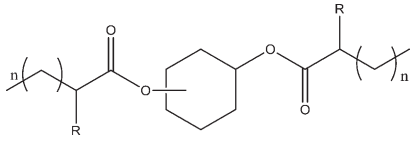 1a–1o			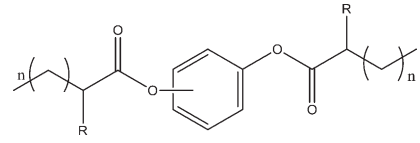 2a–2o		
1a	–H	1	2a	–H	1
1b	–H	3	2b	–H	3
1c	–H	5	2c	–H	5
1d	–H	7	2d	–H	7
1e	$–CH_2CH_3$	3	2e	$–CH_2CH_3$	3
1f	–H	1	2f	–H	1
1g	–H	3	2g	–H	3
1h	–H	5	2h	–H	5
1i	–H	7	2i	–H	7
1j	$–CH_2CH_3$	3	2j	$–CH_2CH_3$	3
1k	–H	1	2k	–H	1
1l	–H	3	2l	–H	3
1m	–H	5	2m	–H	5
1n	–H	7	2n	–H	7
1o	$–CH_2CH_3$	3	2o	$–CH_2CH_3$	3

PREPARATION OF CYCLOHEXANE DIESTER DERIVATIVES (1A–1O) AND BENZENE DIESTER DERIVATIVES (2A–2O)

The analogs of cyclohexane diester or benzene diester were synthesized by esterifying five types of acyl chlorides with six types of diol (i.e., 1,2-cyclohexanediol, 1,3-cyclohexanediol, 1,4-cyclohexanediol, 1,2-benzenediol, 1,3-benzenediol, and 1,4-benzenediol). Ten millimoles of diol was dissolved in 50.0 ml THF, with 12 mmol TEA added slowly. The mixture was stirred for 20 min at room temperature. Then, 12 mmol acryl chloride (butyl chloride, hexanoyl chloride, octanoyl chloride, decanoyl chloride, and 2-ethylhexanoyl chloride) was added and stirred for 6 h at room temperature. Upon completion, the reaction mixture was added to water and extracted with ethyl acetate. The extract was washed with brine, dried over $MgSO_4$, and concentrated under vacuum. The residue was purified by flash column chromatography on a silica gel. Cyclohexane diester derivatives were prepared using the aforementioned general procedure.

MUSHROOM TYROSINASE INHIBITION ASSAY

The inhibitory effect of the test compounds against mushroom tyrosinase was examined using the modified method of Masamoto *et al.* Mushroom tyrosinase (EC 1.14.18.1) used

for the assay was purchased from Sigma-Aldrich. All test compounds dissolved in DMSO to 500 μ*M*. Two hundred and twenty microliters of 0.1 *M* phosphate buffer (pH 6.5), 20 μl of sample solution, and 20 μl of mushroom tyrosinase (2000 units/ml in the same buffer) were mixed in a 96-well microplate, and the mixture was preincubated at 37°C for 5 min. Then, 40 μl of 1.5 m*M* L-tyrosine was added. After incubation at 37°C for 10 min, the absorbance was determined at 490 nm using an ELISA plate reader.

$$\% \text{ Inhibition} = \{(A - b)/A\} \times 100,$$

where A = OD at 490 nm without sample and B = OD at 490 nm with sample.

CELL LINES AND CELL CULTURE

The mouse melanoma cell line, B16F10, was obtained from Korean Cell Line Bank (KCLB, Seoul, Korea). The cells were cultured in DMEM containing 10% FBS, 50 μg/ml penicillin, and streptomycin at 37°C in the humidified atmosphere of 5% CO_2.

CYTOTOXICITY TEST

Cell viability was determined with a modified version of the method published by Tsukahara *et al.* (14) using reduction by thiazolyl blue tetrazolium bromide (MTT). B16F10 cells were seeded in DMEM with 10% FBS in separate 96-well plates at the density of 1×10^4 cells/well before being incubated for 24 h. The test compounds were then added to separate wells, and the cells were incubated for another 24 h, after which 100 μl MTT (300 μg/ml) was added to each well. The cells were incubated for 4 h, and 150 μl DMSO was added to dissolve the formazan crystals. The absorbance of the formazan complexes was measured at 540 nm using an ELISA plate reader.

IN-VITRO MELANIN SYNTHESIS INHIBITION ASSAY

The melanin content of cultured B16F10 cells was determined using a published procedure (7) with slight modifications. The cells were seeded into six-well plates at the density of 3×10^5 cells/well and incubated for 48 h. Each test sample was then added to the cells, which were subsequently incubated for an additional 24 h. The cells were collected by incubation in trypsin-EDTA followed by centrifugation. Cell pellets were dried, dissolved in 1 N NaOH, and boiled for 10 min. After cooling, the absorbance was measured at 400 nm using an ELISA plate reader. The absorbance values of a series of known concentrations of pure melanin were used to construct a calibration curve to determine the amount of melanin produced by the cells.

WESTERN BLOTTING

B16F10 cell lysates were separated by SDS-PAGE (10% polyacrylamide gels) and transferred to polyvinylidene fluoride (PVDF). The membranes were then probed with tyrosinase, TRP-1, TRP-2, and tyrosinase antibodies. Briefly, the cultured B16F10 cells were washed with phosphate-buffered saline and incubated with a RIPA lysis buffer (1% Nonidet P-40, 1%

sodium deoxycholate, 0.1% SDS, 0.15 NaCl, 0.01 *M* sodium phosphate [pH 7.2], 2 m*M* EDTA, 50 m*M* sodium fluoride, 0.2 m*M* sodium orthovanadate, 1 m*M* phenylmethylsulfonyl fluoride, 1 µg/ml aprotinin, and 1 µg/ml leupeptin) for 30 min on ice. Following incubation, the cell lysates were cleared by centrifugation at 15,000 rpm for 30 min, and the resultant supernatants were collected and used to estimate protein concentration by a Bradford assay (15). Then, 10 µg of total protein lysates were resolved on 10% sodium dodecyl sulfate polyacrylamide gels (SDS-PAGE); the separated proteins were transferred to the PVDF membrane. The level of protein expression in each sample was detected using specific primary antibodies, diluted in a TBST solution (Tris-Bufferd Saline and Tween 20) containing 5% (w/v) of skim milk or 3% (w/v) of bovine serum albumin. The membranes were incubated with a specific HRP-conjugated secondary antibody and developed using the enhanced chemiluminescent substrate from West zol-plus. Then, they were stripped and reproved with a β-actin primary antibody as a protein loading control.

REVERSE TRANSCRIPTION-POLYMERASE CHAIN REACTION

The total RNA was extracted from B16F10 cells by using the Trizol reagent (Invitrogen, Carlsbad, CA). After the synthesis of cDNA with oligo $d(T)_{15}$ as a reverse transcriptase primer with the extracted RNA as template, PCR amplification was performed using a GenePro Thermal Cycler (Bioer Technology Co., Ltd, Hangzhou, China). The oligonucleotide primers included (i) tyrosinase: 5′-GGG CCC AAA TTG TAC AGA GA-3′ (upstream) and 5′-GGC AAA TCC TTC CAG TGT GT-3′ (downstream); (ii) TRP-1: 5′-AGG AAT CTG GCT TGG GAT TT-3′ (upstream) and 5′-ATG AGC CAC AAG GGT CAG TC-3′ (downstream); (iii) TRP-2: 5′-AGC AGA CGG AAC ACT GGA CT-3′ (upstream) and 5′-CAG GTA GGA GCA TGA TAG GC-3′ (downstream); and (iv) GAPDH: 5′-AAC TTT GGC ATT GTG GAA GG-3′ (upstream) and 5′-ACA CAT TGG GGG TAG GAA CA-3′ (downstream). The yields of cDNA represented approximately 3 µg of the total input RNA. The reaction was carried out for 35 cycles for 30 s at 94°C, 30 s at 52°C (TRP-1, GAPDH)/53 (TRP-2, tyrosinase), and 30 s at 72°C. The reaction mixtures were analyzed by electrophoresis using 1% agarose gels that were further stained with ethidium bromide. The intensity of the bands was measured using GeneTools software (Syngene, Cambridge, UK).

STATISTICAL ANALYSIS

Mean ± SEM (standard error of the mean) were calculated. Statistical analyses of the results were performed using the *t*-test for independent samples. $p < 0.05$ was considered significant.

A TYROSINASE INHIBITOR MODEL FOR STRUCTURE-BASED DRUG DESIGN

Structure-based drug design is used in assessing changes in protein structure and the interactions (docking) between small-molecule organic compounds. This technique is also employed in the development of new drugs through the use of molecular dynamics.

This study investigated the interactions and the mechanism of whitening by using a tyrosinase inhibitor model and a whitening-derivatives model, the latter being selected based on its whitening effect at the cellular level.

To examine the tyrosinase x-ray crystal structure as a receptor, five tyrosinase structures of *Bacillus megaterium* and *Streptomyces castaneoglobisporus* (protein data bank [PDB] ID: 3NM8, 3NQ1, 1WXC, 2ZWD, 3AWS) were downloaded from the RCSB PDB, and the protein sequences were compared. A homology modeling analysis was performed using the modeler (University of California, San Francisco, CA) focusing on the locations with similar protein sequences. Docking was designed considering the structure of human tyrosinase, which was created by homology modeling using AutoDock Tools (The Scripps Research Institute, La Jolla, CA). Through this program, docking of ligand and target protein was simulated using 3D grid box. The structures of the whitening derivative molecules were generated using the software Cornica (Molecular Networks GmbH, Erlangen, Germany). The process of docking was simulated using the following steps (the same procedure was performed for studying arbutin, another tyrosinase inhibitor):

- Converting 2D structures of whitening derivatives and arbutin into 3D structures.
- Calculating polarities and eliminating water molecules.
- Attaching hydrogen molecules to polar molecules and identifying the location where the ligand of the protein attaches.
- Proceeding with the simulation by using the AutoDock tools.

RESULTS

INHIBITORY EFFECTS OF CYCLOHEXANE DIESTER DERIVATIVES (1A–1O) AND BENZENE DIESTER DERIVATIVES (2A–2O) ON MUSHROOM TYROSINASE ACTIVITY

The mushroom tyrosinase inhibitory activities of cyclohexane diester and benzene diester derivatives were determined using L-DOPA as a substrate. These diester compounds were assayed at a variety of concentrations. However, all compounds showed no inhibitory activities (data not shown).

STRUCTURE–CYTOTOXICITY RELATIONSHIPS OF CYCLOHEXANE DIESTER DERIVATIVES (1A–1O) AND BENZENE DIESTER DERIVATIVES (2A–2O) ON B16F10 CELLS

In an endeavor to identify the structure–cytotoxicity relationships between cyclohexane diester derivatives and benzene diester derivatives in the B16F10 cells, the levels of cytotoxicity were observed in various diester locations (i.e., 1,2-, 1,3-, 1,4-) and by the changing chain length of the acyl group.

The cytotoxicity test results in Table II suggest that, at the concentration of 500 μ*M*, the cytotoxicity of 1,2-cyclohexane diester derivatives and 1,3-cyclohexane diester derivatives increased as the carbon number of the side chain went up. On the other hand, the cytotoxicity of 1,4-cyclohexane diester derivatives tended to decline with the carbon number of the side chain on the rise. In the case of 1,2-benzene diester derivatives, their cytotoxicity decreased with the carbon number of the side chain going up, but then it started increasing from the time when the carbon number of the side chain reached 10 onward. For 1,3-benzene diester derivatives and 1,4-benzene diester derivatives, their cytotoxicity grew lower with an increase in the carbon number of the side chain.

Table II
Viability[a] of Cyclohexane Diester Derivatives (1a–1o) and Benzene Diester Derivatives (2a–2o) on B16F10 Cells

	Viability (%)				
Compounds	25 μ*M*	50 μ*M*	125 μ*M*	250 μ*M*	500 μ*M*
1a	100.0 ± 1.4	96.9 ± 1.9	89.3 ± 1.5	84.2 ± 1.8	70.8 ± 2.1
1b	94.8 ± 1.5	93.0 ± 2.5	86.5 ± 1.8	73.1 ± 1.9	65.0 ± 2.3
1c	100.0 ± 1.8	95.3 ± 1.4	79.6 ± 1.9	66.8 ± 2.5	54.7 ± 1.8
1d	100.0 ± 2.6	94.3 ± 1.6	77.9 ± 0.6	54.5 ± 2.3	40.7 ± 1.8
1e	98.9 ± 1.7	90.7 ± 1.8	73.8 ± 2.6	58.4 ± 2.3	40.1 ± 2.8
1f	100.0 ± 0.4	100.0 ± 3.1	100.0 ± 3.3	94.1 ± 2.2	68.1 ± 3.2
1g	100.0 ± 2.7	100.0 ± 2.4	100.0 ± 1.3	96.9 ± 1.0	74.1 ± 2.7
1h	100.0 ± 2.5	98.1 ± 2.4	91.8 ± 1.4	72.7 ± 3.1	41.0 ± 2.3
1i	100.0 ± 2.1	100.0 ± 2.6	99.3 ± 2.9	99.2 ± 1.6	98.5 ± 1.3
1j	100.0 ± 2.2	100.0 ± 1.1	100.0 ± 1.9	96.1 ± 2.4	96.0 ± 1.8
1k	75.2 ± 1.5	62.1 ± 2.7	57.9 ± 1.6	50.7 ± 1.6	40.2 ± 1.4
1l	91.9 ± 2.1	89.7 ± 0.2	88.8 ± 0.8	85.7 ± 0.9	61.8 ± 1.3
1m	100.0 ± 2.0	100.0 ± 3.1	89.5 ± 2.7	89.5 ± 2.3	79.1 ± 2.4
1n	99.3 ± 3.5	96.8 ± 2.1	95.0 ± 2.2	89.9 ± 3.7	82.4 ± 2.2
1o	93.0 ± 1.2	90.6 ± 0.4	90.0 ± 1.3	87.4 ± 1.7	84.9 ± 1.9
2a	75.6 ± 1.9	64.9 ± 2.4	59.6 ± 3.4	44.3 ± 2.6	7.6 ± 1.5
2b	75.8 ± 0.5	73.1 ± 2.5	59.3 ± 2.8	46.6 ± 2.6	40.2 ± 2.8
2c	93.1 ± 3.0	77.8 ± 3.0	72.3 ± 2.3	61.2 ± 1.8	57.9 ± 2.2
2d	61.3 ± 1.6	58.6 ± 1.3	56.0 ± 2.3	53.0 ± 0.7	48.0 ± 2.7
2e	100.0 ± 2.1	100.0 ± 2.2	100.0 ± 2.5	100.0 ± 2.3	74.3 ± 1.6
2f	92.7 ± 1.0	88.3 ± 1.6	76.8 ± 2.2	65.9 ± 1.8	59.8 ± 2.5
2g	100.0 ± 0.4	98.5 ± 0.6	86.5 ± 1.0	80.6 ± 2.3	62.5 ± 2.3
2h	100.0 ± 2.7	97.4 ± 1.2	94.1 ± 2.1	78.4 ± 2.7	66.9 ± 0.4
2i	100.0 ± 1.4	100.0 ± 2.0	100.0 ± 1.8	99.7 ± 2.4	98.9 ± 2.9
2j	100.0 ± 2.0	100.0 ± 2.1	100.0 ± 2.6	97.7 ± 2.3	94.2 ± 1.2
2k	66.3 ± 1.4	57.5 ± 1.8	34.4 ± 2.3	3.3 ± 0.3	3.2 ± 0.1
2l	49.4 ± 2.6	47.1 ± 2.9	36.2 ± 1.4	21.6 ± 1.5	7.5 ± 0.1
2m	41.5 ± 0.9	33.9 ± 2.1	23.4 ± 0.8	19.8 ± 1.1	18.4 ± 1.1
2n	80.5 ±1.3	78.4 ± 1.4	77.1 ± 0.5	76.4 ± 1.0	74.2 ± 1.5
2o	69.2 ± 1.5	59.3 ± 3.6	58.6 ± 0.5	56.6 ± 1.9	52.9 ± 0.9

[a]Values are means of three experiments.

The results of cytotoxicity tests on octanoyl and 2-ethylhexanoyl—conducted to identify the impact of the structural isomer of the side chain on cytotoxicity—indicate that the levels of cytotoxicity were lower in the branch type than in the linear type across all derivatives except the 1,2-cyclohexane diester derivatives.

When the side chain was the same yet the location of diesters (i.e., 1,2-, 1,3-, 1,4-) varied, the 1,3-diester derivatives demonstrated a lower level of cytotoxicity than the 1,2-diester and 1,4-diester derivatives.

MELANIN SYNTHESIS INHIBITORY EFFECTS OF CYCLOHEXANE DIESTER DERIVATIVES (1A–1O) AND BENZENE DIESTER DERIVATIVES (2A–2O) ON B16F10 CELLS

Table III indicates the melanin synthesis inhibitory activities of cyclohexane diester derivatives (1a–1o) and benzene diester derivatives (2a–2o) in B16F10 cells. As illustrated in the table, the cyclohexane diester derivatives of 1i and 1m and the benzene diester derivative of 2j had 479.3 ± 1.3 μ*M*, 497.9 ± 3.8 μ*M*, and 474.7 ± 9.4 μ*M* as IC_{50} values at the concentration level involving no cytotoxicity. Against this backdrop,

Table III
Melanin Inhibitory Activity[a] of Cyclohexane Diester Derivatives (1a–1o) and Benzene Diester Derivatives (2a–2o) on B16F10 Cells

	Melanin content	
Compounds	% Inhibition at 25 μ*M*	IC_{50} (μ*M*)
1a	0	ND[b]
1b	3.47 ± 0.6	ND
1c	0.42 ± 0.2	ND
1d	0.76 ± 0.7	ND
1e	9.05 ± 1.8	ND
1f	0	ND
1g	0	ND
1h	1.5 ± 1.3	ND
1i	8.8 ± 1.5	479.3 ± 1.3
1j	0	ND
1k	13.4 ± 1.6	ND
1l	0	ND
1m	4.1 ± 0.3	497.9 ± 3.8
1n	0	ND
1o	0	ND
2a	ND	ND
2b	ND	ND
2c	0	ND
2d	ND	ND
2e	2.8 ± 0.2	ND
2f	0	ND
2g	1.5 ± 1.2	ND
2h	0	ND
2i	1.1 ± 0.5	ND
2j	2.3 ± 1.9	474.7 ± 9.4
2k	5.62 ± 0.5	ND
2l	ND	ND
2m	ND	ND
2n	20.7 ± 4.3	ND
2o	ND	ND

[a]Values are means of three experiments.
[b]Not done.

it was concluded that 1i, 1m, and 2j would have whitening effects, and these effects were evaluated at the protein and gene levels through Western blotting and RT-PCR.

WESTERN BLOTTING

Recent reports have demonstrated that many proteins are involved in the regulation of melanin production, including TRP-1, TRP-2, and tyrosinase. To test whether compounds 1i, 1m, and 2j regulated the expression of these proteins, we performed Western blot analysis on B16F10 cells. As shown in Figure 1, treatment with 125 μ*M* compounds 1m and 2j led to significant reduction in the expression of TRP-1 and TRP-2, with a slight decrease in tyrosinase. Also, treatment with 125 μ*M* compound 1i resulted in a slight decrease in TRP-1, TRP-2, and tyrosinase.

EFFECTS OF CYCLOHEXANE DIESTER DERIVATIVES (1I, 1M) AND BENZENE DIESTER DERIVATIVE (2J) ON EXPRESSION OF MRNA IN B16F10 CELLS

To examine whether compounds 1i, 1m, and 2j regulated the expression of those genes, we carried out RT-PCR analysis in B16F10 cells. As portrayed in Figure 2, 1i, 1m, and 2j reduced the expression of mRNA involved in melanin production in a dose-dependent manner. Also, as mentioned in the aforementioned result of Western blotting, treatment with 125 μ*M* compounds, 1i, 1m, and 2j, led to a significant decrease in mRNA such as TRP-1, TRP-2, and tyrosinase.

A TYROSINASE INHIBITOR MODEL FOR STRUCTURE-BASED DRUG DESIGN

As shown in Figure 3, docking with arbutin and benzene diester derivative 2j was identified and was located at the pocket site of human tyrosinase. Figure 4 shows the docking of the benzene diester derivative 2j with five residues, LYS196, PHE209, SER222, ASN226, and VAL239, of human tyrosinase, and docking of arbutin (used for comparison) with three residues, PHE209, ASN226, and HIS22. The results showed the inhibitory effect of benzene diester derivative 2j on human tyrosinase. Benzene diester derivative 2j acted more effectively as a tyrosinase inhibitor than did arbutin. Using this structure-based drug design, further studies on the inhibitory action of cyclohexane diester derivatives 1i and 1m on tyrosinase will be conducted.

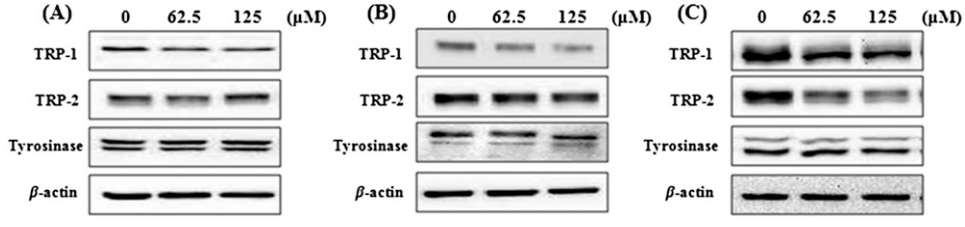

Figure 1. Effects of cyclohexane diester derivatives (1i, 1m) and benzene diester derivative (2j) on expression of protein involved in pigmentation in B16F10 cells. (A) 1i, (B) 1m, and (C) 2j.

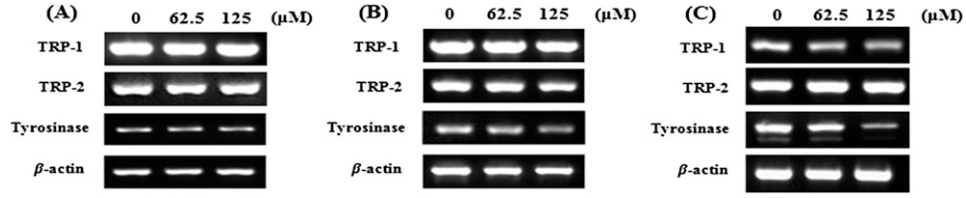

Figure 2. Effects of cyclohexane diester derivatives (1i, 1m) and benzene diester derivative (2j) on expression of mRNA involved in pigmentation in B16F10 cells. (A) 1i, (B) 1m, and (C) 2j.

DISCUSSION

In summary, a novel series of cyclohexane diester derivatives and benzene diester derivatives were prepared and evaluated for the ability to inhibit mushroom tyrosinase and melanin production in B16F10 mouse melanoma cells and were assessed for their structure–cytotoxicity relationships. From the structure–cytotoxicity point of view, it was demonstrated that the binding location of diesters (i.e., 1,2-, 1,3-, 1,4-), change in the carbon number of the side chain, and the difference between the linear and branch types were essential variables for determining cytotoxicity. The melanin inhibitory activities of cyclohexane-1,3-diyl bis(decanoate) (1i), cyclohexane-1,4-diyl dioctanoate (1m), and 1,3-phenylene bis(2-ethylhexanoate) (2j)—having low cytotoxicity while showing whitening effects—were measured at 479.3 ± 1.3 μ*M*, 497.9 ± 3.8 μ*M*, and 474.7 ± 9.4 μ*M*, respectively; their potential as whitening agents were further verified using Western blotting and RT-PCR.

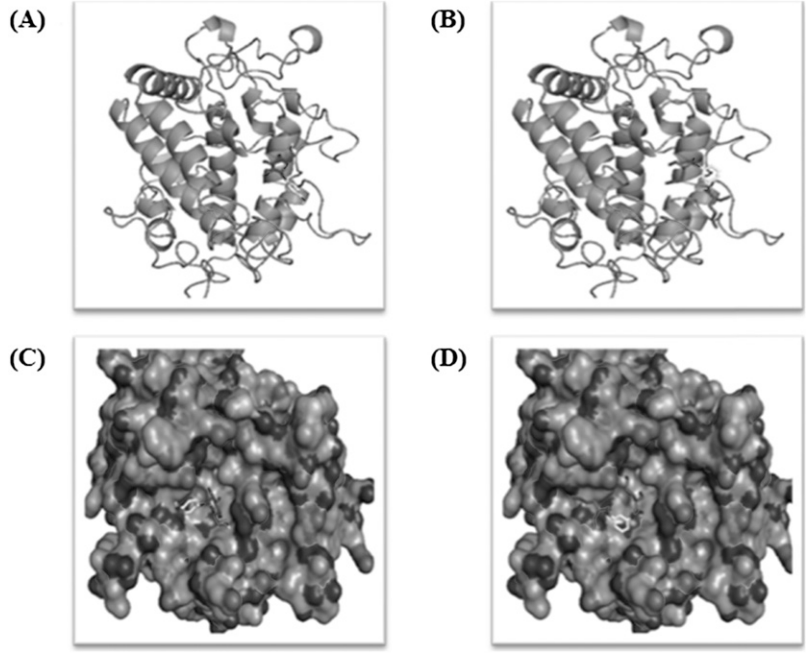

Figure 3. Docking with arbutin and benzene diester derivative (2j) on human tyrosinase. (A) Arbutin docking, (B) 2j docking, (C) cartoon ligand, and (D) surface ligand.

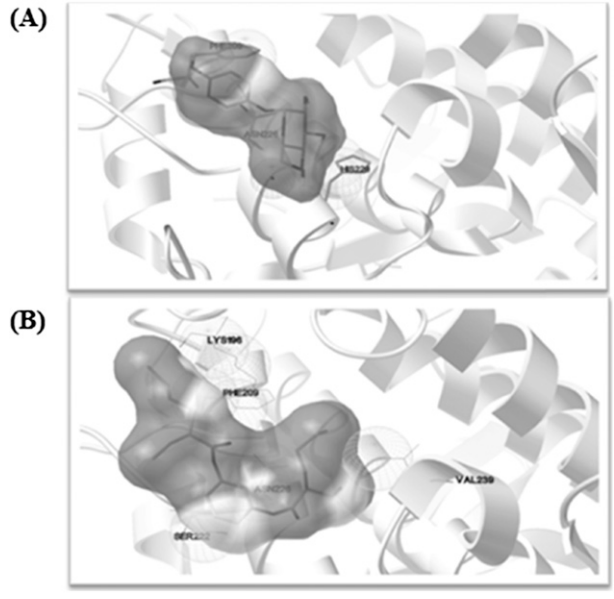

Figure 4. Binding position of arbutin and benzene diester derivative (2j) on human tyrosinase. (A) Arbutin and (B) 2j.

In addition, through the use of a human tyrosinase inhibitor model for structure-based drug design, the inhibitory action of benzene diester derivative 2j on human tyrosinase was established, and thereby the whitening mechanism was also identified. Similar studies on potential whitening agents other than 2j will be undertaken to identify their specific whitening mechanism. In fact, some of them are currently being tested *in-vivo* for whitening effects.

This study on change in cytotoxicity and whitening effects deriving from the structural changes of wide-ranging compounds will contribute to future research on new non-toxic whitening agents.

ACKNOWLEDGMENTS

This study has been sponsored by the Chungcheonbuk-Do Regional Industry R&D Project (A001100495) in the Republic of Korea.

REFERENCES

(1) V. J. Hearing, Biogenesis of pigment granules: A sensitive way to regulate melanocyte function, *J. Dermatol. Sci.,* **37,** 3–14 (2005).
(2) H. Ando, M. S. Matsui, and M. Ichihashi, Quasi-drugs developed in Japan for the prevention or treatment of hyperpigmentary disorders, *Int. J. Mol. Sci.,* **22,** 2566–2575 (2010).
(3) V. M. Virador, N. Kobayashi, J. Matsunaga, and V. J. Hearing, A standardized protocol for assessing regulators of pigmentation, *Anal. Biochem.,* **270,** 207–219 (1999).
(4) E. J. Land, C. A. Ramsden, and P. A. Riley, The mechanism of suicide-inactivation of tyrosinase: A substrate structure investigation, *J. Exp. Med.,* **212,** 341–348 (2007).

(5) C. A. Ramsden, M. R. Stratford, and P. A. Riley, The influence of catechol structure on the suicide-inactivation of tyrosinase, *Org. Biomol. Chem.,* **7,** 3388–3390 (2009).
(6) M. R. Stratford, C. A. Ramsden, and P. A. Riley, Mechanistic studies of the inactivation of tyrosinase by resorcinol, *Bioorg. Med. Chem.,* **21,** 1166–1173 (2013).
(7) M. R. Stratford, C. A. Ramsden, and P. A. Riley, The influence of hydroquinone on tyrosinase kinetics, *Bioorg. Med. Chem.,* **20,** 4364–4370 (2012).
(8) T. Okubo, M. Oyohikawa, K. Futaki, M. Matsukami, and A. Fujii, The inhibitory effects of 4-n-butyl-resorcinol on melanogenesis, *J. Dermatol. Sci.,* **10,** 88 (1995).
(9) O. Nerya, R. Musa, S. Khatib, S. Tamir, and J. Vaja, Chalcones as potent tyrosinase inhibitors: The effect of hydroxyl positions and numbers, *Phytochemistry,* **65,** 1389–1395 (2004).
(10) S. Khatib, O. Nerya, R. Musa, S. Tamir, T. Peter, and J. Vaya, Enhanced substituted resorcinol hydrophobicity augments tyrosinase inhibition potency, *J. Med. Chem.,* **50,** 2676–2681 (2007).
(11) K. Tasaka, C. Kamei, S. Nakano, Y. Takeuchi, and M. Yamato, Effects of certain resorcinol derivatives on the tyrosinase activity and the growth of melanoma cells, *Meth. Find. Exp. Clin. Pharmacol.,* **20,** 99–109 (1988).
(12) K. Shimizu, R. Kondo, and K. Sakai, Inhibition of tyrosinase by flavonoids, stilbenes and related 4-substituted resorcinols: Structure-activity investigations, *Planta Med.,* **66,** 11–15 (2000).
(13) H. Oozeki, R. Tajima, and K. Nihei, Molecular design of potent tyrosinase inhibitors having the bibenzyl skeleton. *Bioorg. Med. Chem. Lett.,* **18,** 5252–5254 (2008).
(14) K. Tsukahara, Y. Takema, S. Moriwaki, N. Tsuji, Y. Suzuki, T. Fujimura, and G. Imokawa, Selective inhibition of skin fibroblast elastase elicits a concentration-dependent prevention of ultraviolet B-induced wrinkle formation, *J. Invest. Dermatol.,***117,** 671–677 (2001).
(15) M. M. Bradford, A dye binding assay for protein, *Anal. Biochem.,* **72,** 248–254 (1976).

J. Cosmet. Sci., **65,** 187–195 (May/June 2014)

Stability of urea in solution and pharmaceutical preparations

NATTAKAN PANYACHARIWAT and HARTWIG STECKEL,
Department of Pharmaceutics and Biopharmaceutics, Christian Albrecht University of Kiel, 24118 Kiel, Germany.

Accepted for publication March 10, 2014.

Synopsis

The stability of urea in solution and pharmaceutical preparations was analyzed as a function of temperature (25°–60°C), pH (3.11–9.67), and initial urea concentration (2.5%–20%). This study was undertaken to (i) obtain more extensive, quantitative information relative to the degradation of urea in both aqueous and non-aqueous solutions and in pharmaceutical preparations, and (ii) test the effects of initial urea concentration, pH, buffer, and temperature values on urea degradation. The stability analysis shows that urea is more stable at the pH range of 4–8 and the stability of urea decreases by increase in temperature for all pH values. Within the experimental range of temperature and initial urea concentration values, the lowest urea degradation was found with lactate buffer pH 6.0. The urea decomposition rate in solution and pharmaceutical preparations shows the dependence of the initial urea concentrations. At higher initial urea concentrations, the rate of degradation is a decreasing function with time. This suggests that the reverse reaction is a factor in the degradation of concentrated urea solution. For non-aqueous solvents, isopropanol showed the best effort in retarding the decomposition of urea. Since the losses in urea is directly influenced by its stability at a given temperature and pH, the stability analysis of urea by the proposed model can be used to prevent the loss and optimize the operating condition for urea-containing pharmaceutical preparations.

INTRODUCTION

Being widely used in pharmaceutical and cosmetic products, urea plays a vital role in maintaining the skin's moisture balance and suppleness. Reduced levels of urea, representing 7% of the natural moisturizing factors in the stratum corneum (skin-building layer), lead to a lower water-binding capacity within the skin, which in turn, results in roughness, tightness, flaking, and irritation of the skin. Urea preparations typically range in strength from 3 to 20, in specific preparations up to 40%, and can take many forms, including creams, gels, shampoos, deodorants, foundation, and even toothpaste.

Ever since the decomposition of urea was first presented by Wöhler in 1829 (1), the understanding of its products, by-products, and reaction pathways has been extensively the subject of several studies over the past century (2–11), but little information exists relative to the stability of urea in non-aqueous solutions and pharmaceutical preparations. Urea

Address all correspondence to N. Panyachariwat at npanyachariwat@pharmazie.uni-kiel.de and H. Steckel at hsteckel@pharmazie.uni-kiel.de.